



## 저작자표시 2.0 대한민국

이용자는 아래의 조건을 따르는 경우에 한하여 자유롭게

- 이 저작물을 복제, 배포, 전송, 전시, 공연 및 방송할 수 있습니다.
- 이차적 저작물을 작성할 수 있습니다.
- 이 저작물을 영리 목적으로 이용할 수 있습니다.

다음과 같은 조건을 따라야 합니다:



저작자표시. 귀하는 원저작자를 표시하여야 합니다.

- 귀하는, 이 저작물의 재이용이나 배포의 경우, 이 저작물에 적용된 이용허락조건을 명확하게 나타내어야 합니다.
- 저작권자로부터 별도의 허가를 받으면 이러한 조건들은 적용되지 않습니다.

저작권법에 따른 이용자의 권리는 위의 내용에 의하여 영향을 받지 않습니다.

이것은 [이용허락규약\(Legal Code\)](#)을 이해하기 쉽게 요약한 것입니다.

[Disclaimer](#) 

A THESIS  
FOR THE DEGREE OF MASTER OF SCIENCE

Endothelium dependent vasorelaxation  
of Gallic acid isolated from *Spirogyra* sp.  
and its antihypertension effect

Nalae Kang

Department of Marine Life Science  
GRADUATE SCHOOL  
JEJU NATIONAL UNIVERSITY  
FEBRUARY, 2013

Endothelium dependent vasorelaxation  
of Gallic acid isolated from *Spirogyra* sp.  
and its antihypertension effect

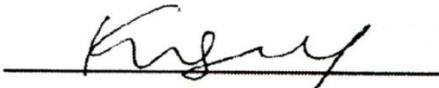
**Nalae Kang**  
(Supervised by **Professor You-Jin Jeon**)

A thesis submitted in partial fulfillment of the requirement  
for the degree of Master of Science  
2013. 02.

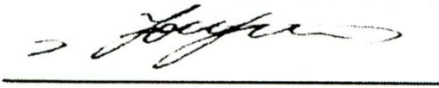
This thesis has been examined and approved by



Thesis director, Seunghoon Lee, Professor of Marine Life Science



Gi-Young Kim, Professor of Marine Life Science



You-Jin Jeon, Professor of Marine Life Science

2013. 02.

Date

Department of Marine Life Science  
GRADUATE SCHOOL  
JEJU NATIONAL UNIVERSITY

## CONTENTS

국문초록 .....	iii
LIST OF FIGURES .....	v
LIST OF TABLES .....	vii
ABSTRACT .....	1
INTRODUCTION .....	3
MATERIALS AND METHODS .....	6
Materials .....	6
Preparation of ethyl acetate fraction of <i>Spirogyra</i> sp. (SPE) .....	6
Procedure of CPC .....	7
Cell culture .....	8
Cell viability .....	9
Assay of nitric oxide (NO) levels .....	9
Immunoblotting .....	10

Measurement of intracellular calcium levels .....	10
Procedure of HPLC .....	11
In silico docking of proteins and new inhibitor candidate.....	11
Statistical analysis .....	12
<b>RESULTS AND DISCUSSION .....</b>	<b>13</b>
NO production by influx of calcium into HUVECs .....	13
Isolation of five fractions from ethyl acetate fraction of <i>Spirogyra</i> sp. (SPE) .....	18
NO production of SPE.IV in HUVECs .....	20
SPE.IV induces influx of calcium into HUVECs .....	26
Identification of SPE.IV .....	28
In silico docking of Phosphodiesterase 5 (PDE5) .....	30
Angiotensin-I Converting Enzyme (ACE) inhibitory activity of gallic acid (GA) .....	34
<b>CONCLUSION .....</b>	<b>39</b>
<b>REFERENCES .....</b>	<b>40</b>
<b>ACKNOWLEDGEMENT .....</b>	<b>45</b>

## 국문초록

순환계는 신체의 모든 기관으로 산소와 영양분을 운반하는 역할을 하는 기관계이며, 순환계에서 혈관은 매우 중요한 조직이다. 혈관의 항상성이 유지되지 않을 경우에는 고혈압, 심근경색, 동맥경화 등의 심각한 심혈관계 질환에 노출된다. 이러한 질환에 직·간접적인 영향을 미치는 혈관확장은 혈관의 이완 운동에 따라 일어나는 현상이다. 혈관은 크게 평활근 세포와 내피 세포로 이루어져 있는데, 평활근 세포가 이완 운동을 하고, 내피 세포는 평활근 세포가 운동할 수 있도록 신호를 전달한다. 내피 세포에 의존적인 혈관확장 신호 물질 중에서 가장 중요한 것은 산화질소이다. 내피 세포에 존재하는 endothelial Nitric Oxide Synthase (eNOS)에서 생성된 산화질소는 평활근 세포로 확산되어 cyclic Guanosine Monophosphate (cGMP)를 생성시킴으로써 혈관을 확장시킨다.

본 연구에서는 수생식물인 해캄에서 분리한 에틸아세테이트 층의 혈관확장 효과를 인형 제대정맥 내피세포에서 확인하였다. 해캄 에틸아세테이트 층은 고성능 원심분배 크로마토그래피를 통하여 분리되었으며, 분리된 물질들의 혈관확장 효과는 산화질소 생성, eNOS의 인산화, 내피세포로의 칼슘의 유입과 같은 내피 세포에 의존적인 요인들을 측정함으로써 확인하였다.

해캄 에틸아세테이트 층에서 분리한 물질들 중에서 SPE.IV 는 유의적으로 내피 세포에 의존적인 혈관확장 효과를 나타내었으며, eNOS의 저해제인 N<sup>G</sup>-nitro-L-arginine methyl

ester (L-NAME)를 전처리 할 경우, SPE.IV에 의한 혈관확장 효과가 저해되는 것을 확인하였다. LC/MS 및  $^1\text{H}$  NMR data 를 비교·분석한 결과, SPE.IV는 항산화제로 널리 알려진 갈산임을 확인하였다.

평활근 세포에서 갈산의 혈관확장 효과는 분자 모델링 연구를 통하여 cGMP를 분해하는 효소인 Phosphodiesterase 5 (PDE 5)에 대한 결합 작용을 예측·분석하였다. 그 결과, 갈산은 비교적 안정적으로 PDE 5의 활성 부위에 결합함으로써 효소의 cGMP 분해 작용을 억제하는 것으로 예측된다.

혈관확장과 관련된 질환인 고혈압은 동맥경화, 뇌졸중, 심근경색 등의 합병증 발병의 원인이 되는 심각한 만성 질환이다. 본 연구에서는 혈관확장과 더불어 갈산의 항고혈압 활성을 확인하기 위해서 안지오텐신 I 전환 효소의 저해 활성을 평가하였다. 그 결과,  $122.9\ \mu\text{g/ml}$ 의  $\text{IC}_{50}$  value 을 나타내어 비교적 우수한 활성을 나타내는 것을 확인하였다. 효소 저해 패턴을 예측·분석하기 위해 분자 모델링 연구를 수행한 결과, 효소의 활성 부위의 입구를 막음으로써 안지오텐신 I 전환 효소의 작용을 저해하는 것으로 예측된다.

결론적으로 갈산은 혈관확장 효과와 항고혈압 효과를 동시에 가짐으로써 혈관 질환 개선의 효과를 나타낼 것으로 사료된다.

## LIST OF FIGURES

Figure 1. Fluorescent intensity of intracellular calcium levels after treatment of CaCl<sub>2</sub> in HUVECs. Values are mean  $\pm$  SD of three determinations. Values are significantly different at  $P < 0.01$  as analyzed by DMRT.

Figure 2. Fluorescent image of intracellular calcium levels after treatment of CaCl<sub>2</sub> in HUVECs.

Figure 3. NO levels (A) and cell viability (B) after treatment of CaCl<sub>2</sub> in HUVECs. NO levels were measured after staining with DAF-FM DA.

Figure 4. Isolation of ethyl acetate fractions of *Spirogyra* sp. (SPE).

Figure 5. NO production (A) and cell viability (B) of SPE fractions in HUVECs. Values are mean  $\pm$  SD of three determinations. Values are significantly different at  $P < 0.01$  as analyzed by DMRT.

Figure 6. NO production of SPE.IV in HUVECs. NO levels were measured after staining with DAF-FM DA. Values are mean  $\pm$  SD of three determinations. Values are significantly different at  $P < 0.01$  as analyzed by DMRT.

Figure 7. Inhibition of L-NAME on NO production of SPE.IV in HUVECs. NO levels were measured after staining with DAF-FM DA. Values are mean  $\pm$  SD of three



determinations. Values are significantly different at  $P < 0.01$  as analyzed by DMRT.

Figure 8. Effect of SPE.IV on eNOS, iNOS and Akt expression in HUVECs. Equal amounts of cell lysates (10  $\mu\text{g}$ ) were subjected to electrophoresis and analyzed for diverse protein related in NO production such as phospho-eNOS(Ser 1177), phospho-Akt (Ser 473).  $\beta$ -actin was used as an internal control.

Figure 9. Fluorescent intensity of intracellular calcium levels with treatment of SPE.IV in HUVECs. Values are mean  $\pm$  SD of three determinations. Values are significantly different at  $P < 0.1$  as analyzed by DMRT.

Figure 10. Identification of Gallic acid (GA)

Figure 11. Computational prediction of the structure for PDE 5 and docking simulation with GA. Predicted 3D structure of PDE 5 (PDB ID : 1UDT). 2D diagram (PDE 5-GA complex).

Figure 12. ACE inhibitory activity of GA isolated from *spirogyra* sp.

Figure 13. Computational prediction of the structure for ACE and docking simulation with GA. Predicted 3D structure of ACE (PDB ID : 1O86). 2D diagram (ACE-GA complex).

## **LIST OF TABLES**

Table 1. Results of docking experiments of GA with the PDE5 (PDB ID: 1UDT)

Table 2. Results of docking experiments of GA with the ACE (PDB ID: 1O86)

## ABSTRACT

In the present study, vasorelaxation effect of ethyl acetate fraction of aquatic plant, *Spirogyra* sp. was investigated using human umbilical vein endothelial cells (HUVECs). *Spirogyra* sp. ethyl acetate fraction (SPE) was isolated through high performance centrifugal partition chromatography (HPCPC), and identified its vasorelaxation effect by measuring endothelium dependent factors including nitric oxide (NO) levels, phosphorylation of endothelial Nitric Oxide Synthase (eNOS) and influx of calcium into HUVECs.

Among the SPE fractions, SPE.IV significantly induced endothelium dependent vasorelaxation. Moreover, this vasorelaxation effect induced by SPE.IV was attenuated by pretreatment with N<sup>G</sup>-nitro-L-arginine methyl ester (L-NAME), eNOS inhibitor. SPE.IV was identified as gallic acid (GA) by comparing LC/MS and 1H NMR data to the literature report.

Vasorelaxation effect of GA in vascular smooth muscle cell was evaluated by simulating binding mode of GA to Phosphodiesterase 5 (PDE 5), enzyme interrupting vasorelaxation, using the crystal structure of PDE 5 (PDB ID: 1UDT). The molecular modeling study was successful (calculated binding energy value: -90.00 kcal/mol), suggested that GA interacts with Phe820, Gln817 and Ser663.

Hypertension directly related with vasorelaxation is the most common serious chronic disease because it is a high risk factor for arteriosclerosis, stroke, and myocardial infarction (Je et al., 2005).

Antihypertensive effect of GA was estimated as angiotensin-I converting enzyme (ACE) inhibitory activity using ACE kit (DOJINDO Laboratories, Kumamoto Japan). GA exhibited relatively high ACE inhibitory activity with  $IC_{50}$  value of 122.9  $\mu\text{g/ml}$ . For further insight, binding mode of GA to ACE using the crystal structure of ACE (PDB ID: 1O86). The molecular modeling study was successful (calculated binding energy value: -128.33 kcal/mol), suggested that GA interacts with Glu384, Tyr523, Ala356 and Arg522.

Therefore, GA could be a profound enhancer on vascular diseases by possessing endothelium-dependent vasorelaxation effect and antihypertensive effect.

## 1. INTRODUCTION

Blood vessels are vital tissue of the circulatory system which transports oxygen and nutrients to all vertebrate organs, supporting organ development as well as metabolism and homeostasis (Villasenor et al., 2012). Blood vessels consist of endothelial cells, the inner lining of vessels, and smooth muscle cells, within the vessel walls (Golpon et al., 2003). Vasorelaxation is relaxation of smooth muscle cells and is an important physiological phenomenon related in various vascular diseases such as hypertension, myocardial infarction and atherosclerosis even erectile dysfunction. Vasorelaxation improves these vascular diseases by alleviating high blood pressure and peripheral resistance (Shou et al., 2012).

Mechanism of vasorelaxation is various and may be exerted in endothelium-dependent and/or-independent manners (Akhlaghi et al., 2009). In the endothelium-dependent relaxation effect, endothelial cells regulate the function of the underlying vascular smooth muscle cells and the diameter of the vessels (Kim et al., 2011).

The endothelium-dependent relaxation effect is mediated by nitric oxide (Akhlaghi et al., 2009). NO is generated via oxidation of L-arginine catalyzed by NO synthase (NOS), which exists in three isoforms: inducible NOS (iNOS), endothelial NOS (eNOS) and neuronal NOS (nNOS) expressed in a variety of tissues (Alderton et al., 2001, Jin et al., 2011).

Depending on isoforms of NOS, generated NO plays respectively different role. NO generated by iNOS is a critical player in the development of various airway inflammatory diseases and is a part of complex signaling systems associated with airway inflammatory diseases. (Lee et al., 2010). On the other hands, NO generated by eNOS is an endothelium-derived messenger molecule and plays an important role in the control of cardiovascular homeostasis by maintaining coronary vasodilatory tone, inhibiting platelet aggregation and inhibiting adhesions of neutrophils and platelets to vascular endothelium (Akhlaghi et al., 2009). After  $Ca^{2+}$ /calmodulin pathways, NO generated in Endothelial cells diffuses to vascular smooth muscle cells and increases intracellular cyclic Guanosine Monophosphate (cGMP) with activation of the soluble guanylyl cyclase (sGC), leading to relaxation of underlying vessels (Rapoport and Murad, 1983, Jin et al., 2011).

Hypertension caused by vasoconstriction has become a worldwide major problem threat to human health. It is the most common serious chronic health problem, because it is a high risk factor for arteriosclerosis, stroke, and myocardial infarction (Je et al., 2005).

Angiotensin I-converting enzyme (ACE) performs a pivotal function in the regulation of blood pressure (Lee et al., 2009). ACE converts an inactive form of decapeptide, angiotensin I (Asp-Arg-Val-Tyr-Ile-His-Pro-Phe-His-Leu), to octapeptide angiotensin II (Asp-Arg-Val-Tyr-Ile-His-Pro-Phe), a potent vasoconstrictor, and inactivates bradykinin, which exerts a depressor effect (Je et al., 2005).

ACE inhibition has been used extensively in therapeutic strategies for the prevention and treatment of hypertension. Several synthetic ACE inhibitors have been developed, including alacepril, captopril, benazepril, enalapril, fosinopril, ramipril, and zofenopril, all of which are currently extensively used in the treatment of essential hypertension and heart failure in humans (Ondetti et al., 1997). However, these synthetic ACE inhibitors are believed to exert certain side effects, including cough, taste disturbances, and skin rashes (Kato et al., 1972). Therefore, the development of ACE inhibitors from natural products has become a major area of research.

In this study, vasorelaxation effect of ethyl acetate fractions of aquatic plant, *Spirogyra* sp. was investigated using human umbilical vein endothelial cells (HUVECs) and vascular smooth muscle cell. Moreover, its antihypertension, caused by vasoconstriction, effect was investigated on ACE inhibitory activity.

## 2. MATERIALS AND METHODS

### 2.1. Materials

Antibodies including phospho-eNOS (Ser1177), iNOS and phospho-Akt (Ser473) were purchased from Cell signaling Technology (Beverly, MA). Calcium flux assay kit was purchase from BD Biosciences. Diamino fluorophore 4-amino-5-methylamino-2',7'-difluorofluorescein diacetate (DAF-FM DA) and N<sup>G</sup>-nitro-L-arginine methyl ester (L-NAME) was purchase from Sigma Chemical Co. (St. Louis, MO, USA). The other chemicals and reagents used were of analytical grade.

### 2.2. Preparation of ethyl acetate fraction of *Spirogyra* sp. (SPE)

*Spirogyra* sp. was collected from several shallow pond in Kongju, Korea (36°20'34", 127°12'28"). Samples were cleaned and cultured in modified Bold's Basal Medium at 20°C under 50 µmol photons m<sup>-2</sup>s<sup>-1</sup> (12L/12D) for 3years, and ground and shifted through a 50 mesh standard testing sieve after dried by freeze dryer SFDSMO6, and then dried *Spirogyra* sp. was stored in refrigerator until use.

Dried *Spirogyra* sp. (20 g) was extracted three times for 3hrs using 80% MeOH under



sonication at room temperature. The extract was concentrated in a rotary vacuum evaporator and partitioned with ethyl acetate, and then the dried ethyl acetate fraction was stored in a refrigerator for CPC separation.

### **2.3. Procedure of CPC**

The CPC experiments were performed using a two-phase solvent system composed of ethyl acetate/methanol/water (10:1:9, v/v). The two phases were separated after thoroughly equilibrating the mixture in a separating funnel at room temperature. And, for dual mode operation, the upper organic phase was used as the stationary phase (0~150 min) and mobile phase (150~300 min), whereas the lower aqueous phase was employed as the mobile phase (0~150 min) and stationary phase (150~300 min).

The CPC column was initially filled with the organic stationary phase and then rotated at 1000 rpm while the mobile phase was pumped into the column in the descending mode at the flow rate used for the separation (2 mL/min) and makes change to ascending mode after 150 min. When the mobile phase emerged from the column, indicating that hydrodynamic equilibrium had been reached (back pressure : 2.1 MPa), The concentrated ethyl acetate fraction (500 mg) from the 80% MeOH extracts from *S. varians* was dissolved in 6 mL of a

1:1 (v/v) mixture of the two CPC solvent system phases and was injected through the Rheodyne injection valve. The effluent from the CPC was monitored in the UV at 254 nm and fractions were collected with 6 mL in 8mL tube by a a Advantec CHF 122SC fraction collector (Toyo seisakusho kaisha LTD., Japan).

#### **2.4. Cell culture**

Human umbilical vein endothelial cells (HUVECs) and endothelial cell basal medium-2 (EBM-2) with endothelial cell growth medium-2 (EGM-2) bullet kit were purchased from Clonetics Inc. (San Diego, USA). Cells were maintained in culture at 37 °C in a humidified atmosphere containing 5% CO<sub>2</sub>, in EBM-2 supplemented with ascorbic acid, 2% fetal bovine serum (FBS), hydrocortisone, human fibroblast growth factor (hFGF), vascular endothelial growth factor (VEGF), human epidermal growth factor (hEGF), long R insulin-like growth factor-1 (R3-IGF-1), gentamicin sulfate (CA-1000) and heparin as described by the manufacturer. Cells were employed between passage 3 and 6.

#### **2.5. Cell viability**

Cell viability was quantified through a colorimetric MTT assay that measured the mitochondrial

activity in viable cells. Cells ( $1 \times 10^5$  cells/mL) in 96-well plates were incubated without or with the sample of various concentrations (25 and 50  $\mu\text{g/ml}$ ) for 1.5 h prior to MTT treatment. 50  $\mu\text{L}$  of MTT stock solution (2 mg/mL in PBS) was added to each well. After incubation of 4 h, the plates were centrifuged for 10 min at 2000 rpm and the supernatants were aspirated. The formazan crystals in each well were dissolved in DMSO. The amount of purple formazan was assessed by measuring the absorbance at 540 nm.

## **2.6. Assay of nitric oxide (NO) levels**

Generation of NO was analyzed using a fluorescent probe dye, diaminofluorophore 4-amino-5-methylamino-2',7'-difluorofluorescein diacetate (DAF-FM DA) which is converted via a NO-specific mechanism to an intensely fluorescent triazole derivatives (Itoh et al., 2000). Cells ( $1 \times 10^5$  cells/mL) in 96-well plates were incubated without or with the sample of indicated concentrations for 1.5 h. Then, DAF-FM DA solution (5  $\mu\text{M}$ ) was treated and cells were incubated at 37  $^{\circ}\text{C}$  for 1 h in the dark. After incubation, fluorescence was measured using a fluorescence plate reader.

## **2.7. Immunoblotting**

Phospho-eNOS, iNOS and phospho-Akt (Ser473) expressions were determined by western blot analysis (Yamabe et al., 2007). Total protein (10 ug) levels were electrophoresed through 12% sodium dodecyl sulfate–polyacrylamide gel. Separated proteins were transferred electrophoretically to a pure nitrocellulose membrane, blocked with 5% skim milk solution for 2 h, and then incubated with primary antibodies overnight at 4 °C. After washing of the blots, they were incubated with goat anti-rabbit or goat anti-mouse IgG HRP conjugated secondary antibody for 1 h at room temperature. Signals were developed using an enhanced chemiluminescence (ECL) western blotting detection kit and exposed to X-ray films.

## **2.8. Measurement of intracellular calcium levels**

Intracellular calcium levels were analyzed using the BD™ Calcium Assay Kit. Cells ( $1 \times 10^5$  cells/mL) in 96-well plates were incubated without or with the sample of indicated concentrations for 1.5 h. Then, loading solution was treated and the cells were incubated at 37 °C for 1 h in the dark as described by the manufacturer. After incubation, fluorescence was measured using a fluorescence plate reader. The images of the cells were observed using a fluorescent microscope, which was equipped with a Moticam color digital camera (Motix, Xiamen, China).

## **2.9. Procedure of HPLC**

The HPLC system in this experiment consisted of two mono Waters 515 HPLC pump, a Waters 2998 photodiode array detector, Waters 2707 autosampler, and Waters pump control module II (Waters, USA). A 10  $\mu$ L of 5 mg/ml sample solution was directly injected on Atlantis T3 3 $\mu$ m 3.0 X 150mm column (Waters, USA) using a gradient acetonitrile–water solvent system. The mobile phase was acetonitrile – water in gradient mode as follows: acetonitrile with 0.1% formic acid – water with 0.1% formic acid (0 min ~ 40 min : 5:95 v/v ~ 50:50 v/v, ~ 50 min : ~ 100: 0 v/v, ~ 60min : ~ 100:0 v/v). The flow rate was 0.2 mL/min with UV absorbance detection at 254 nm.

## **2.10. In silico docking of proteins and new inhibitor candidate**

Molecular docking is an application that molecular modeling techniques are used to predict how a protein (enzyme) interacts with small molecules (ligands) (Perola E. 2006). The ability of a protein to interact with small molecules plays a major role in the dynamics of that protein, which may enhance or inhibit its biological function (Kang et al., 2012)

For docking studies, the crystal structures of protein were allocated from Protein Data Bank (PDB, <http://www.pdb.org>). The docking studies were performed using CDOCKER in Accelrys Discovery Studio 3.0 (Accelrys, Inc). To prepare for the docking procedure, we performed the following steps:

(1) conversion of the 2D structure into 3D structure; (2) calculation of charges; and (3) addition of hydrogen atoms using the CDocker docking program.

### **2.11. Statistical analysis**

All data were expressed as mean  $\pm$  standard deviation (SD) of three determinations. Statistical comparison was performed via a one-way analysis of variance (ANOVA) followed by Duncan's multiple range test (DMRP). P-values of less than 0.01 ( $P < 0.01$ ), 0.05 ( $P < 0.05$ ) and 0.1 ( $P < 0.1$ ) was considered as significant.

### **3. Results and Discussion**

#### **3.1. NO production by influx of calcium into HUVECs.**

To experimentally identify whether calcium flow into the cell and then NO was produced, we measured intracellular calcium levels and NO levels after treatment of CaCl<sub>2</sub> to HUVECs. As shown in fig. 1, fluorescent intensity of intracellular calcium increase compared with non treatment, although the difference of value is small and it is not concentration-dependent manner. Calcium play an important role in the physiology and biochemistry of organisms and cells such as signal transduction pathways, neurotransmitter release from neurons, contraction of all muscle cell types and fertilization. However, calcium levels in mammals are tightly regulated. Martin et al. (2002) studied that calcium influx to endothelial cells and appeared amount of calcium as nM (Martin et al.,2002). Likewise, fluorescent intensity of intracellular calcium in fluorescent image is slightly increased when CaCl<sub>2</sub> was treated at relative high concentration (30~50 µg/ml) (Fig. 2).

Moreover, NO levels produced by treatment of CaCl<sub>2</sub> increased compared with non treatment, although it is not concentration-dependent manner as well as intracellular calcium levels (Fig. 3).

As a result, the fact that calcium inflow to endothelial cells and then NO is produced was experimentally verified.

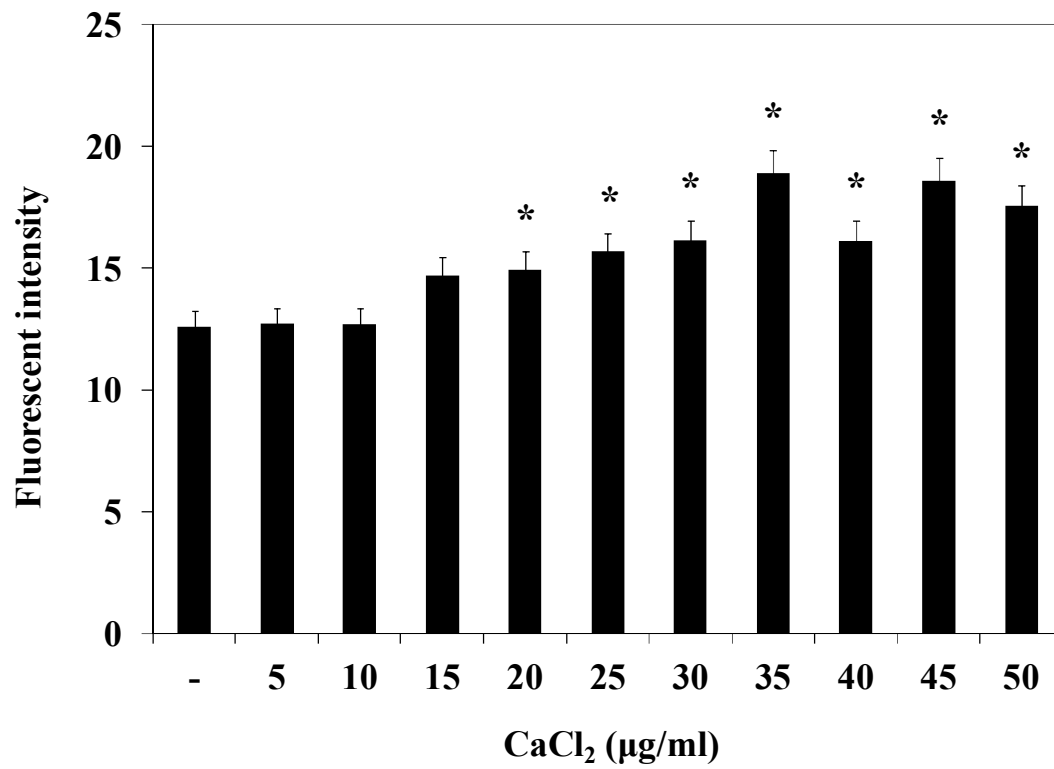


**Figure 1. Fluorescent intensity of intracellular calcium levels after treatment of CaCl<sub>2</sub> in HUVECs. Values are mean  $\pm$  SD of three determinations. Values are significantly different at P < 0.01 as analyzed by DMRT.**



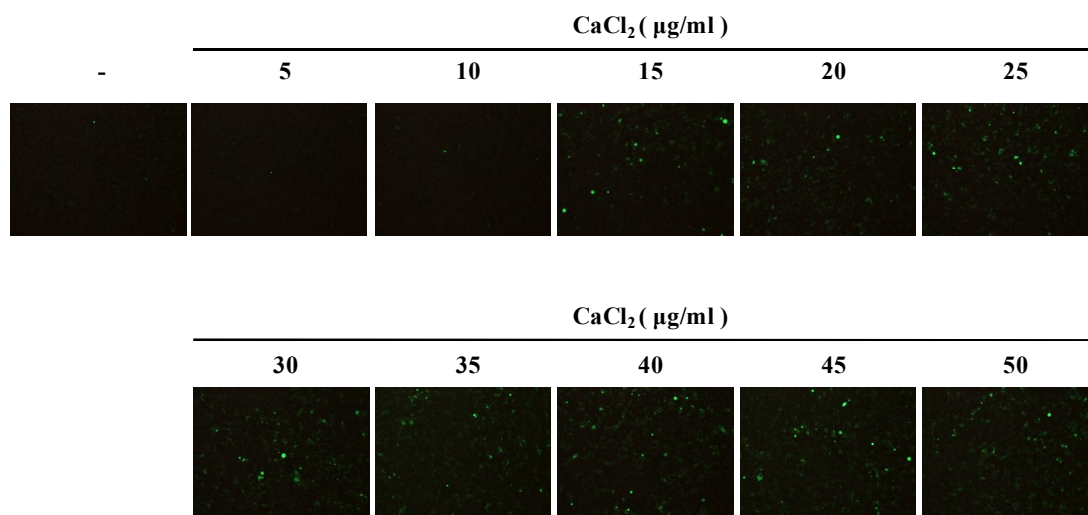


**Figure 2. Fluorescent image of intracellular calcium levels after treatment of CaCl<sub>2</sub> in HUVECs.**

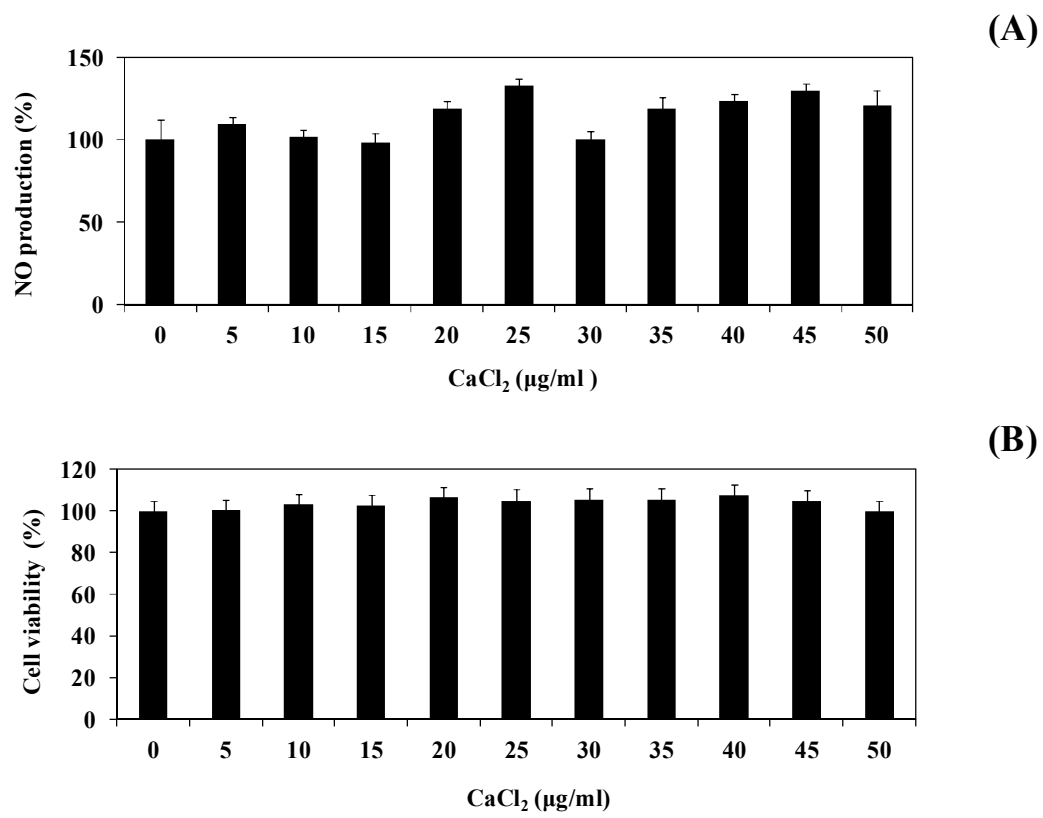


**Figure 3. NO levels (A) and cell viability (B) after treatment of CaCl<sub>2</sub> in HUVECs. NO levels were measured after staining with DAF-FM DA.**

### **3.2. Isolation of five fractions from ethyl acetate fraction of *Spirogyra* sp. (SPE)**

The five fractions (SPE.I~V, respectively) were successfully isolated from SPE by CPC with a two-phase solvent system composed of n-hexane / EtOAc / methanol / water (0:10:1:9, v/v) exhibited good K values for dual mode operation (Fig. 4).

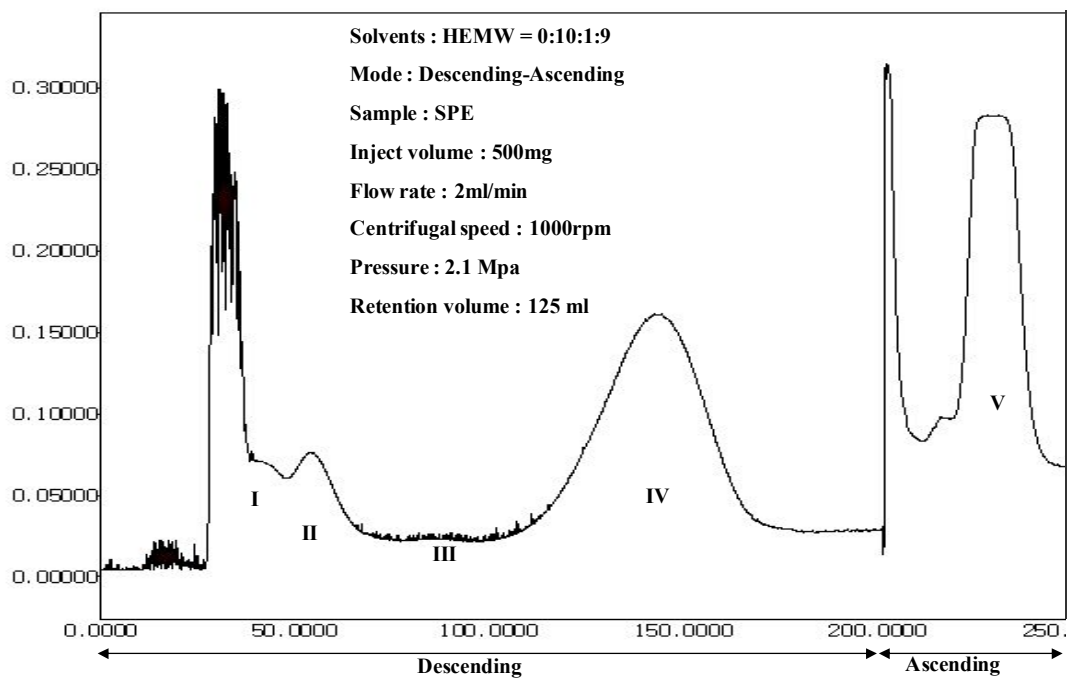


Figure 4. Isolation of ethyl acetate fraction of *Spirogyra* sp. (SPE)

### **3.3. NO production of SPE.IV in HUVECs.**

Among the signaling molecule in relation to vasorelaxation, NO production is most important (Akhlaghi et al., 2009, Woldman et al., 2009). To identify vasorelaxation effect of SPE fractions in HUVECs, first of all, NO production was examined.

As shown in Fig. 5, most of fractions not showed the cytotoxicity at dose of 25, 50  $\mu\text{g/ml}$  excluding the SPE.V (Fig. 5 (B)) meanwhile NO level in SPE.IV-treated HUVECs was significantly increased at 25, 50  $\mu\text{g/ml}$  compared with other fractions (Fig. 5 (A)). Therefore, SPE.IV was taken for the further experiments.

To identify the effect of SPE.IV in HUVECs, we measured that NO production of SPE.IV-treated HUVECs with different concentrations. As shown in Fig. 6, SPE.IV significantly increased NO levels in a concentration-dependent manner at doses of 12.5, 25, 50 and 100  $\mu\text{g/ml}$ .

Moreover, in order to exactly confirm whether NO production of SPE.IV related with endothelial nitric oxide synthase (eNOS), N<sup>G</sup>-nitro-L-arginine methyl ester (L-NAME), eNOS inhibitor, was pretreated to HUVECs. In consequence, NO levels increased by SPE. IV was significantly attenuated by L-NAME at a concentration of 100  $\mu\text{M}$ . Therefore, NO produced by SPE.IV in HUVECs is induced through eNOS.

To investigate whether SPE.IV influences eNOS protein expression levels, HUVECs was incubated

with SPE.IV of 25 µg/ml. As shown in Fig 8, no change on the eNOS protein levels however, p-eNOS (Ser 1177) expression level was increased in SPE.IV-treated HUVECs than in non-treated HUVECs. On the other hands, iNOS expression level was little higher in SPE.IV-treated HUVEC than in non-treated HUVECs but the difference has not influence on NO production. Therefore, SPE.IV induced NO production though phosphorylation of eNOS.

eNOS can be phosphorylated by other kinases such as phosphoinositol 3-kinase (PI3K)/Akt (Mount et al., 2007). To investigate whether SPE.IV influences Akt protein expression levels during eNOS phosphorylation by SPE.IV, HUVEC was incubated with SPE.IV of 25 µg/ml and western blotting analysis was performed. As shown in Fig 8, SPE.IV induced the phosphorylation of Akt (Ser473) at 25 µg/ml.

As a result, the increase of NO production by SPE.IV in HUVECs is mediated through the phosphorylation of eNOS (Ser 1177) via phosphorylation of Akt (Ser473).

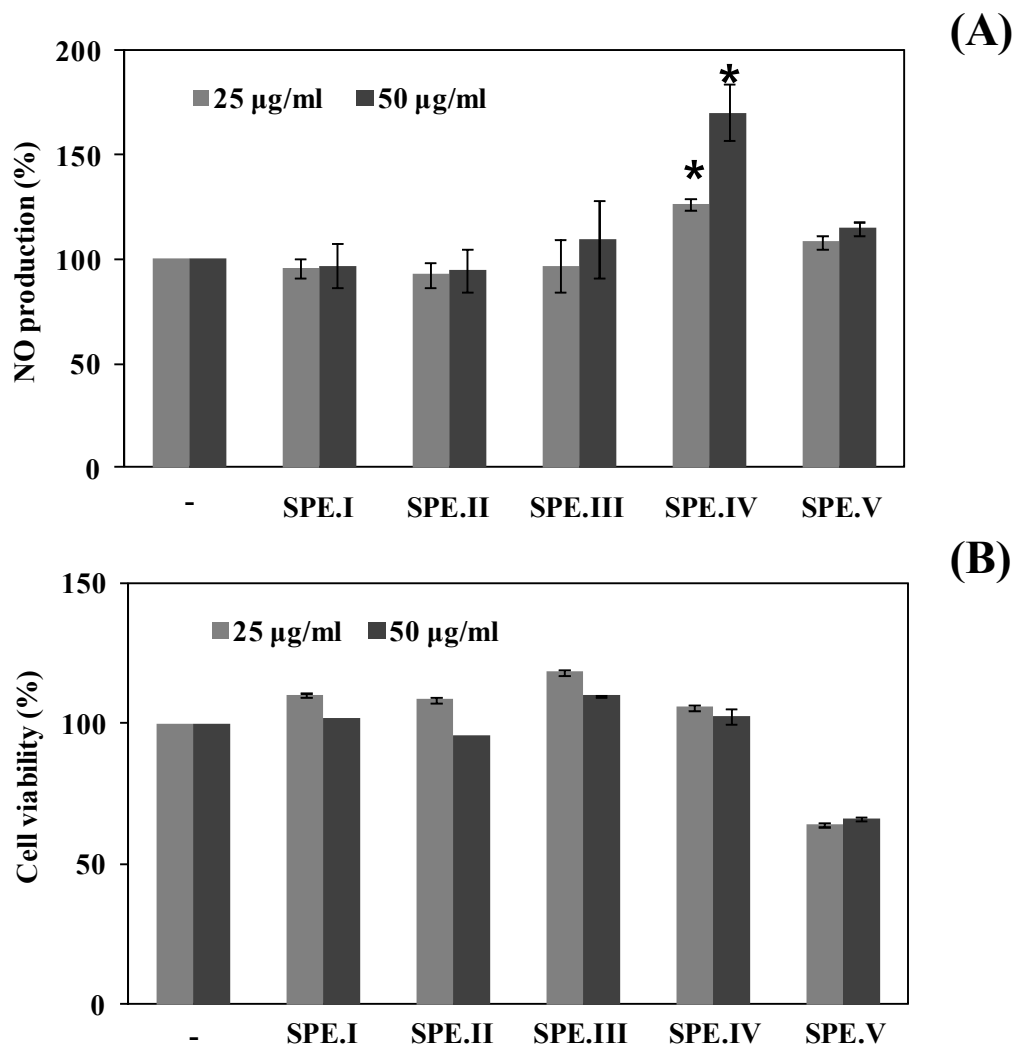


**Figure 5. NO production (A) and cell viability (B) of SPE fractions in HUVECs. Values are mean  $\pm$  SD of three determinations. Values are significantly different at  $P < 0.01$  as analyzed by DMRT.**

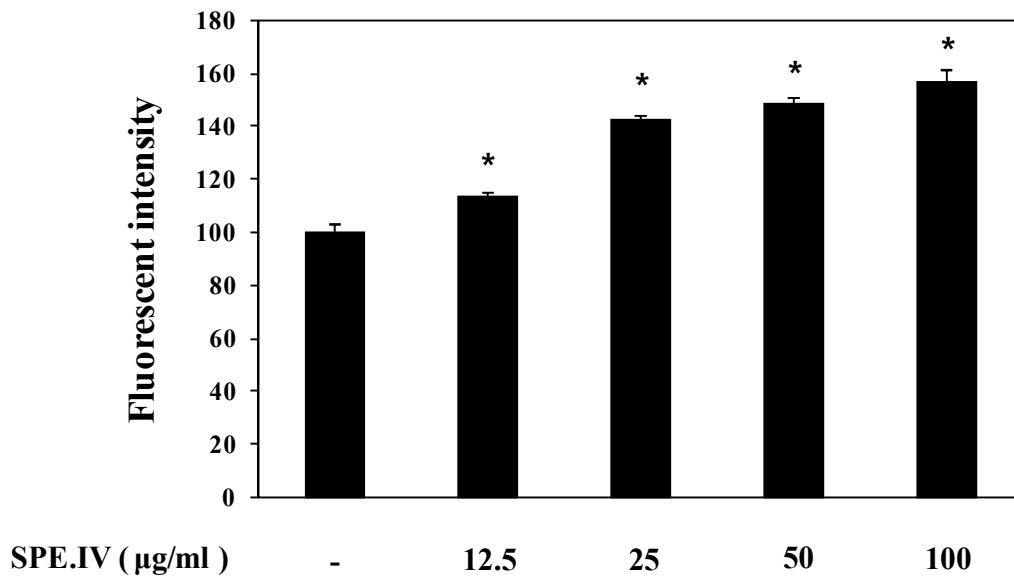


**Figure 6. NO production of SPE.IV in HUVECs. NO levels were measured after staining with DAF-FM DA. Values are mean  $\pm$  SD of three determinations. Values are significantly different at  $P < 0.01$  as analyzed by DMRT.**



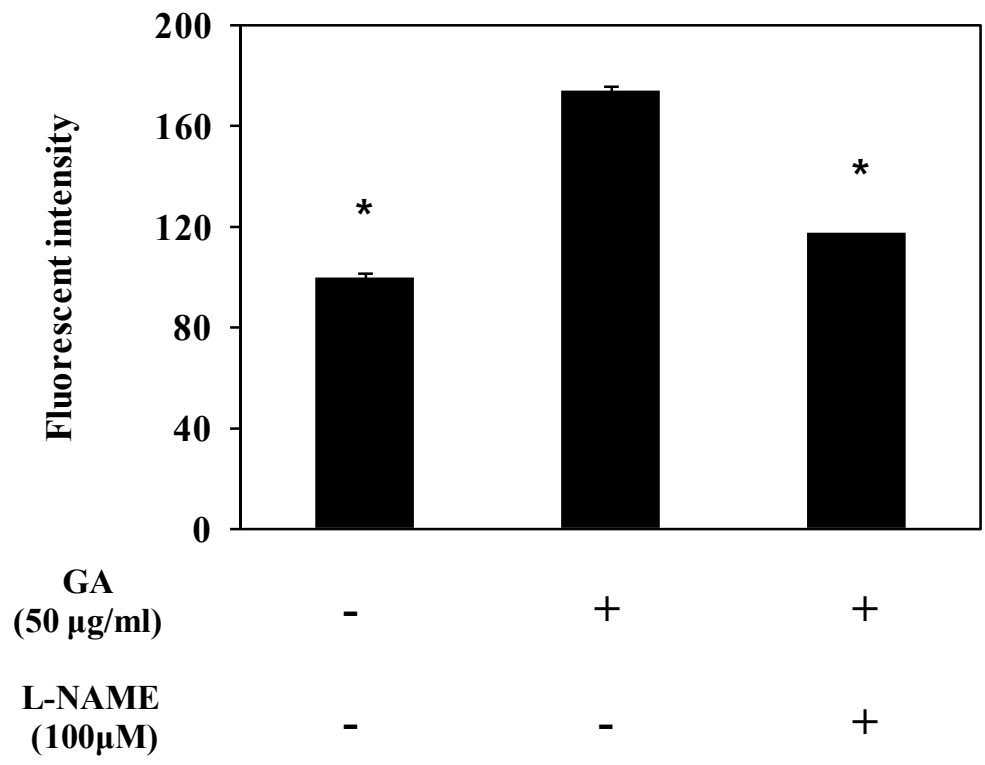


**Figure 7. Inhibition of L-NAME on NO production of SPE.IV in HUVECs. NO levels were measured after staining with DAF-FM DA. Values are mean ± SD of three determinations. Values are significantly different at P < 0.01 as analyzed by DMRT.**

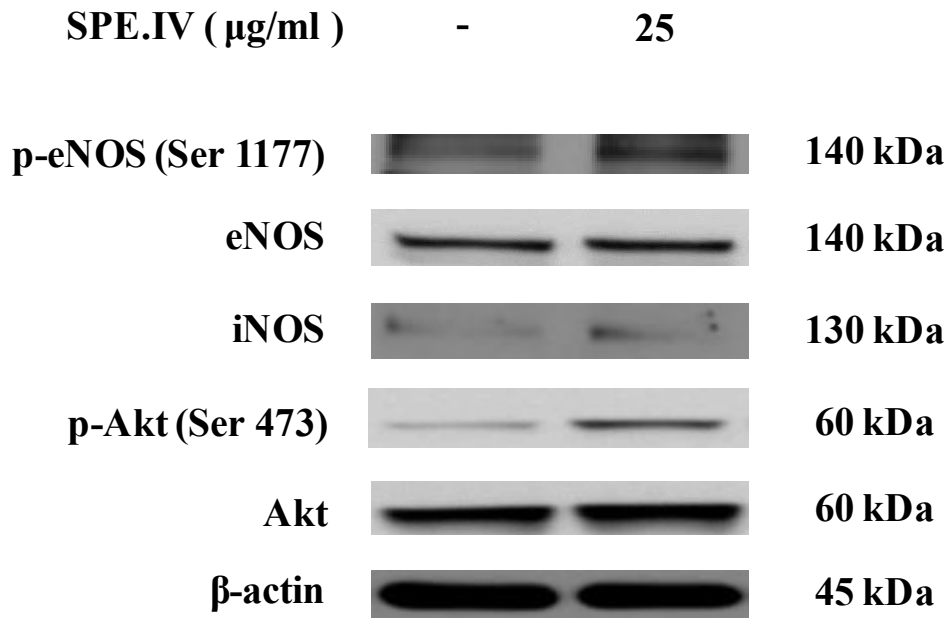


**Figure 8. Effect of SPE.IV on eNOS, iNOS and Akt expression in HUVECs. Equal amounts of cell lysates (10  $\mu\text{g}$ ) were subjected to electrophoresis and analyzed for diverse protein related in NO production such as phospho-eNOS(Ser 1177), phospho-Akt (Ser 473).  $\beta$ -actin was used as an internal control.**

### **3.4. SPE.IV induces influx of calcium into HUVECs**

eNOS is a calcium-dependent enzyme (Akhlaghi et al., 2009). In order to evaluate the direct role of SPE.IV on the regulation of intracellular calcium levels, we incubated HUVECs with SPE.IV of 12.5, 25 and 50  $\mu\text{g/ml}$  and measured intracellular calcium levels using the BD<sup>TM</sup> Calcium Assay Kit. The intracellular calcium levels were increased in SPE.IV-treated HUVECs, although it is not significant (Fig. 9). Therefore, NO production of SPE.IV-treated HUVECs was induced by influx of calcium.

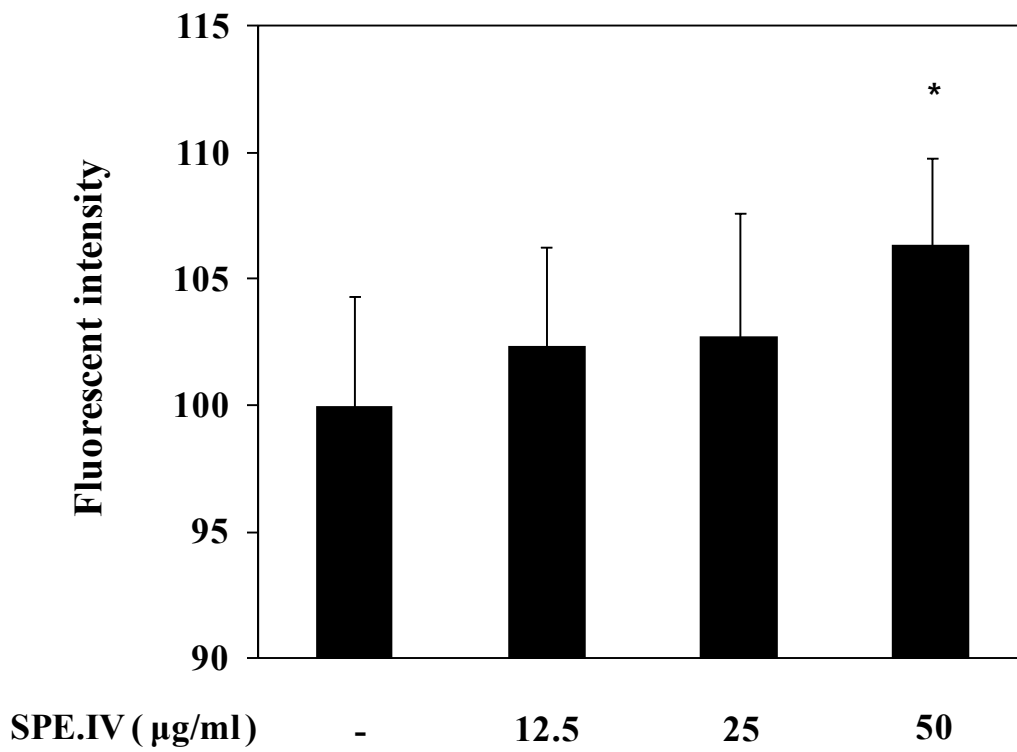
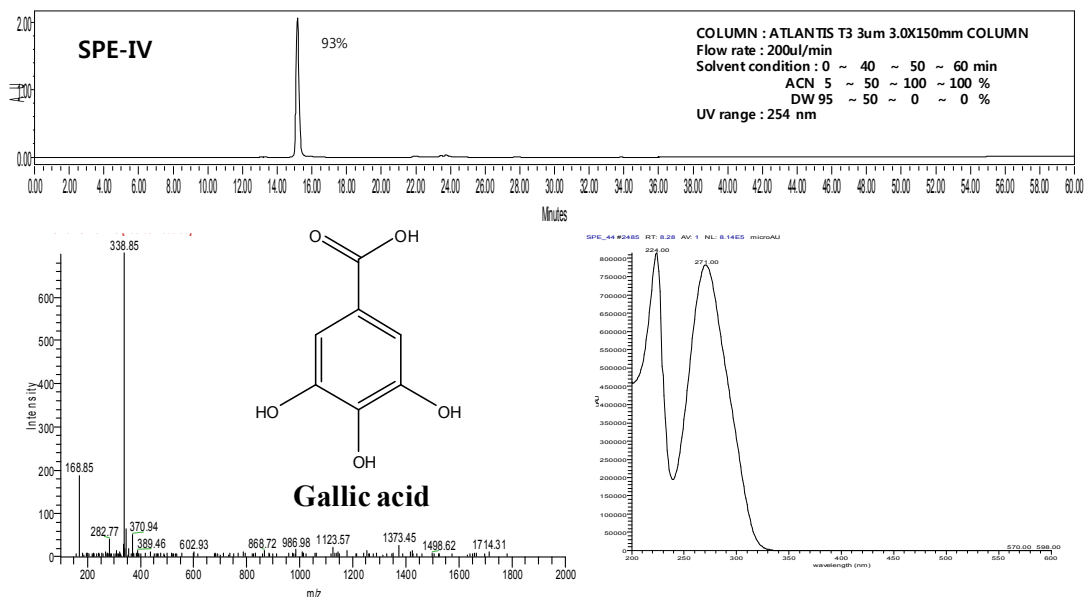


**Figure 9. Fluorescent intensity of intracellular calcium levels with treatment of SPE.IV in HUVECs. Values are mean  $\pm$  SD of three determinations. Values are significantly different at  $P < 0.1$  as analyzed by DMRT.**

### 3.5. Identification of SPE.IV

SPE.IV mass values and UV spectra by LC-DAD-ESI/MS, SPE.IV was identified as gallic acid ( $m/z$  170) (Fig. 10). The structural identification of gallic acid was carried out by  $^1\text{H}$  NMR and  $^{13}\text{C}$  NMR spectra as follows: gallic acid:  $^1\text{H}$  NMR (400 MHz, methanol- $d_4$ )  $\delta$  7.05(2H, s, H-2, 6);  $^{13}\text{C}$  NMR (400 MHz, methanol- $d_4$ ):  $\delta$  169.9(-COOH),  $\delta$  145.5(C-3, 5),  $\delta$  138.5(C-4),  $\delta$  121.7(C-1),  $\delta$  109.4(C-2, 6).



<sup>1</sup>H NMR (400 MHz, methanol-d<sub>4</sub>) δ 7.05(2H, s, H-2, 6); <sup>13</sup>C NMR (400 MHz, methanol-d<sub>4</sub>): δ 169.9(-COOH), δ 145.5(C-3, 5), δ 138.5(C-4), δ 121.7(C-1), δ 109.4(C-2, 6).

**Figure 10. Identification of Gallic acid (GA)**

### 3.6. In silico docking of Phosphodiesterase 5 (PDE 5)

Phosphodiesterases (PDEs) are a class of enzymes that cleave the phosphodiester bond in cyclic adenosine monophosphate (cAMP) and cyclic guanosine monophosphate (cGMP) which relaxes smooth muscle, resulting in vasorelaxation. (Rahimi et al., 2010, Sung et al., 2003, Schwartz et al., 2012). PDEs inhibitors are the drugs targets for the medical management of diverse physiological dyfunctions including heart failure, depression, asthma, inflammation and erectile dysfunction (Sung et al., 2003).

Of the 12 PDE families, cGMP-specific PDE 5 carries out the principal cGMP-hydrolysing activity in human corpus cavernosum tissue. It is well known as the target of sildenafil citrate (Viagra) and other similar drugs for the treatment of erectile dysfunction (Sung et al., 2003).

The PDE 5 inhibition mode of the GA was predicted by molecular docking analysis. To simulate docking of the protein-ligand complex, Discovery Studio 3.0 (DS) was utilized. For docking studies, the crystal structure of PDE 5 was allocated from Protein Data Bank (PDB ID : 1UDT) and active site of PDE 5 involved the following residues : Phe820, Gly819, Gln 817, Met816, Leu804, Ala783, Ala779 and Tyr664.

The docking of the PDE 5-ligand complexes was well-performed with GA stably posed in the pocket of the PDE 5 by DS 3.0 (Fig. 11). The binding site predicted by the 2D program of DS 3.0 (Fig. 11)

was formed by the following residues : Phe820 (pi interaction bond), Gln817 (hydrogen bond) and Ser663 (hydrogen bond). Moreover, the docking analysis results indicated that the following highest docking binding energy and lowest total binding energy confirmation of the most proposed complex had to be taken into account when using the CDOCKER interaction energy program of DS 3.0: 22.91 kcal/mol and in the calculate program of DS 3.0: -90.00 kcal/mol (Table 1).



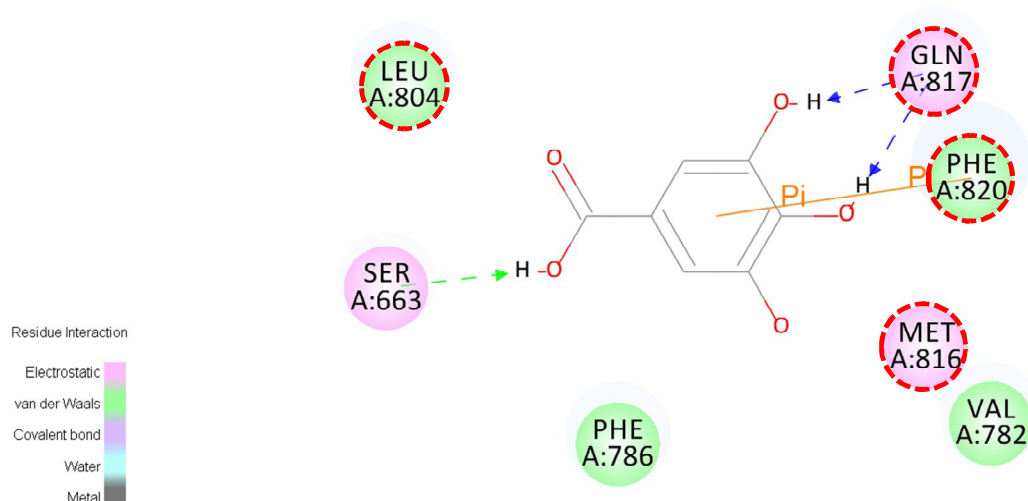
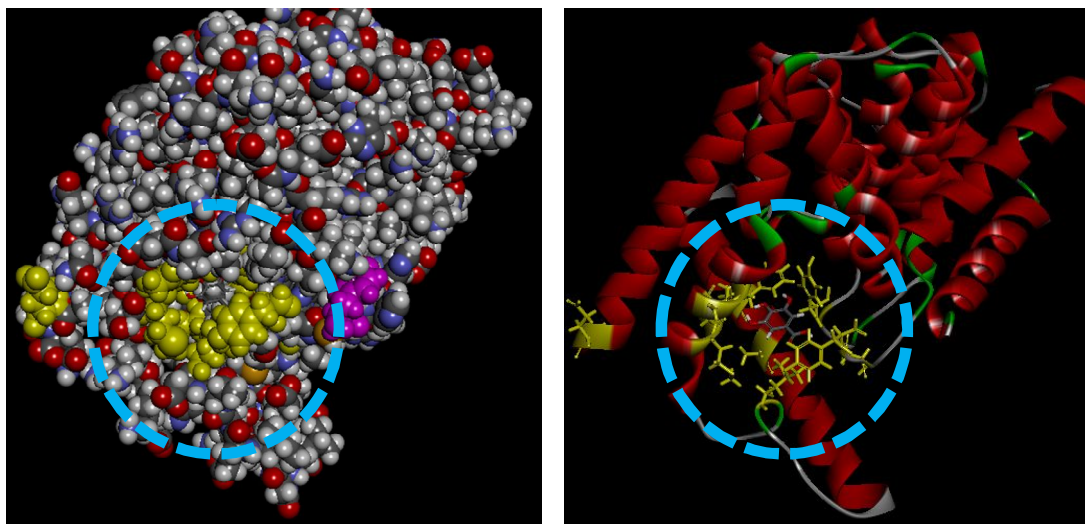


**Figure 11. Computational prediction of the structure for PDE 5 and docking simulation with GA. Predicted 3D structure of PDE 5 (PDB ID : 1UDT). 2D diagram (PDE 5-GA complex).**

**Table 1. Results of docking experiments of GA with the PDE5 (PDB ID: 1UDT)**

Ligand	Binding energy (kcal/mol)	CDOCK interaction energy (kcal/mol)
Gallic acid	-90.00	22.91

### **3.7. Angiotensin-I Converting Enzyme (ACE) inhibitory activity of gallic acid (GA)**

Antihypertensive treatment with Angiotensin-I Converting Enzyme (ACE) inhibitors can improve endothelium-dependent vasorelaxation (Clozel, Kuhn and Hefti, 1990). The most potent improvement of endothelium function might be obtained by ACE inhibitors, and reduce blood pressure by inhibiting not only the production of angiotensin II, but also via the degradation of bradykinin, the vasorelaxation activity of which is caused by NO (Asselbergs et al., 2005).

The antihypertensive effect of GA was evaluated by measuring Angiotensin I converting enzyme (ACE) inhibitory activity using ACE kit (Dojindo). As shown in Figure 12, GA showed the relatively high activity with an  $IC_{50}$  value of 122.9  $\mu\text{g/mL}$ .

The ACE inhibition mode of the GA was predicted by molecular docking analysis. To simulate docking of the protein-ligand complex, Discovery Studio 3.0 (DS) was utilized. For docking studies, the crystal structure of ACE was allocated from Protein Data Bank (PDB ID : 1O86) and active site of ACE involved the following residues : Tyr520, His513, Tyr523, Lys511, Gln281, Glu411, His353, Glu162, Ala354, His383, Glu384, His387

The docking of the ACE-ligand complexes were well-performed by blocking the active site pocket of the ACE by DS 3.0 (Fig. 13). The binding site predicted by the 2D program of DS 3.0 (Fig. 12) was formed by the following residues : Tyr523 (hydrogen bond), Glu384 (hydrogen bond). Moreover,

the docking analysis results indicated that the following highest docking binding energy and lowest total binding energy confirmation of the most proposed complex had to be taken into account when using the CDOCKER interaction energy program of DS 3.0: 45.62 kcal/mol and in the calculate program of DS 3.0: -128.33 kcal/mol (Table 2).

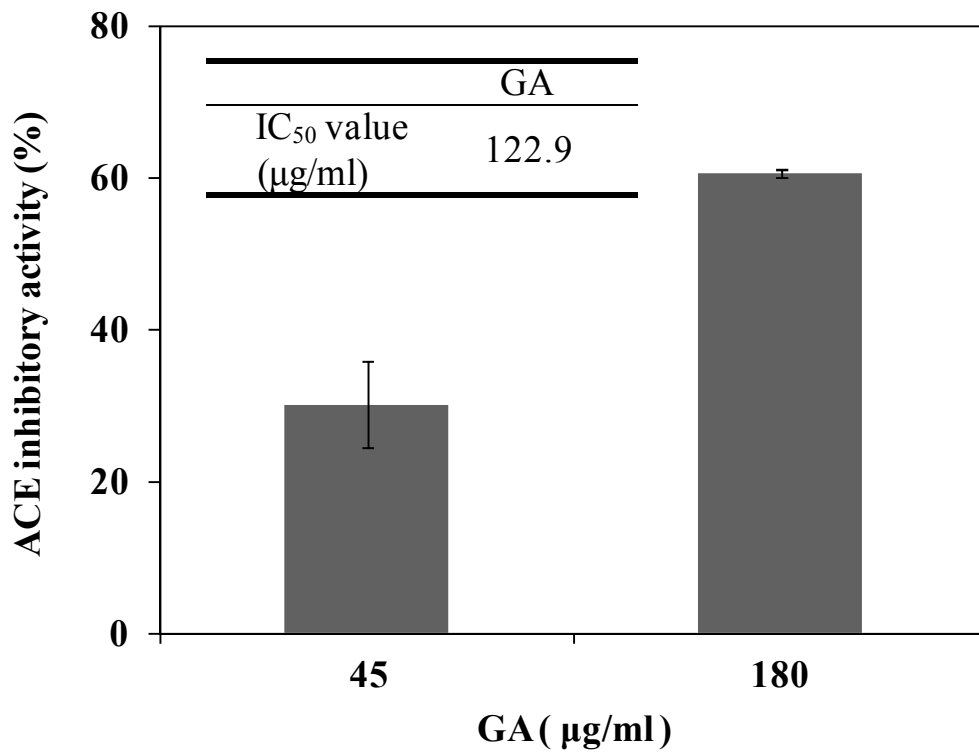
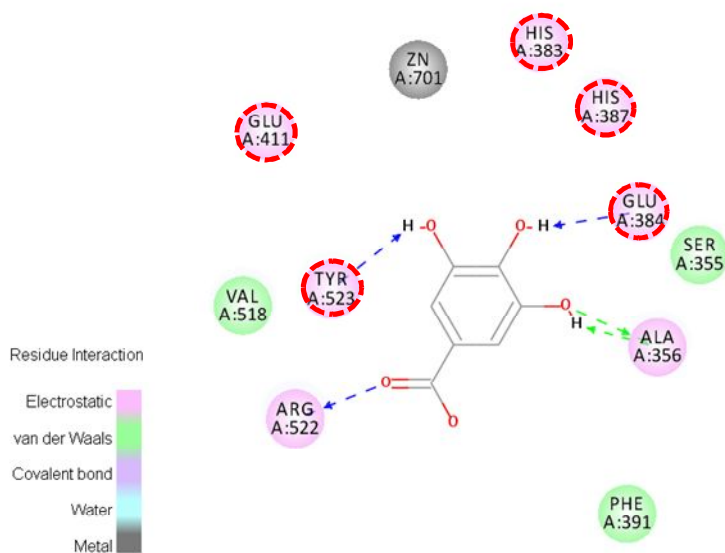
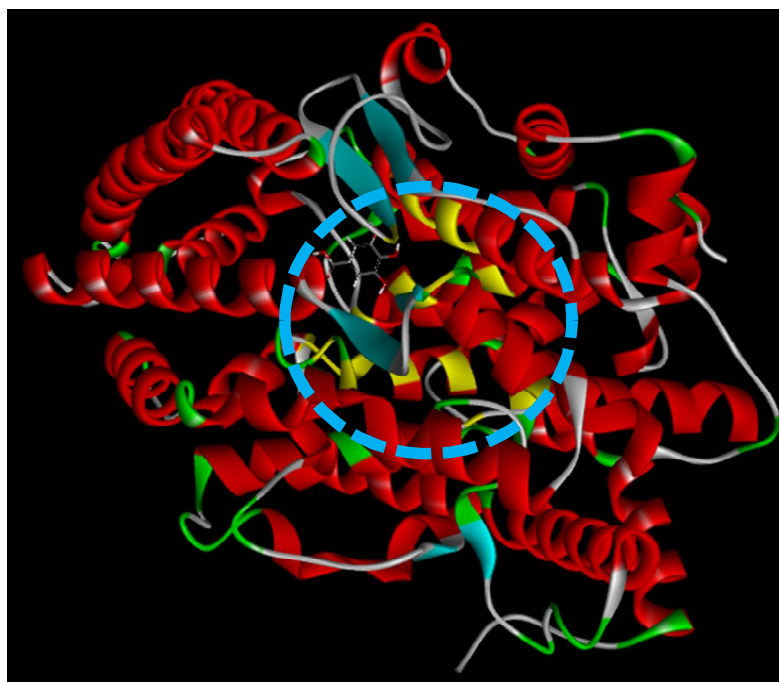


Figure 12. ACE inhibitory activity of GA isolated from *spirogyra* sp. Values are mean  $\pm$  SD of three determinations. Values are significantly different at  $P < 0.01$  as analyzed by DMRT.



**Figure 13. Computational prediction of the structure for ACE and docking simulation with GA.**

**Predicted 3D structure of ACE (PDB ID : 1O86). 2D diagram (ACE-GA complex).**

**Table 2. Results of docking experiments of GA with the ACE (PDB ID:1O86)**

Ligand	Binding energy (kcal/mol)	CDOCK interaction energy (kcal/mol)
Gallic acid	-128.33	45.62

## 4. Conclusion

In this study, we investigated vasorelaxation effect of GA isolated from the aquatic plant, *Spirogyra* sp. Our results demonstrate that the profound vasorelaxation effect of GA on NO production in HUVECs. Vasorelaxation effect of the GA is mediated through the phosphorylation of eNOS (Ser 1177) via phosphorylation of Akt (Ser473). Also, PDE 5 inhibition effect of the GA was predicted through molecular docking program (DS 3.0). Also, the GA possesses antihypertensive effect related with vasorelaxation. Therefore, GA is considered profound enhancer on vascular diseases by exhibiting vasorelaxation and antihypertension effect, simultaneously.



## REFERENCES

- Akhlaghi M, Bandy B. (2009) Mechanisms of flavonoid protection against myocardial ischemia-reperfusion injury. *J. Mol. Cell. Cardiol.* 46: 309-317
- Chen CC, Ke WH, Ceng LH, Hsieh CW, Wung BS. (2010) Calcium- and phosphatidylinositol 3-kinase/Akt-dependent activation of endothelial nitric oxide synthase by apigenin. *Life Sci.* 87:743-749
- Clozel M, Kuhn H, Hefti F. (1990) Effects of Angiotensin Converting Enzyme Inhibitors and of Hydralazine on Endothelial Function in Hypertensive Rats. *Hypertension.* 16: 532-540
- Golpon HA, Puchner A, Barth P, Welte T, Wichert PV, Feddersen CO. (2003) Nitric oxide-dependent vasorelaxation and endothelial cell damage caused by mercury chloride. *Toxicology.* 192: 179-188
- Heo SJ, Hwnag JY, Choi JI, Lee SH, Park PJ, Kang DH, Oh C, Kim DW, Han JS, Jeon YJ, Kim HJ, Choi IW. (2010) Protective effect of diphlorethohydroxycarmalol isolated from *Ishige okamurae* against high glucose-induced-oxidative stress in human umbilical vein endothelial cells. *Food Chem. Toxicol.* 48: 1448-1454
- Hung LM, Su MJ, Chen JK. (2004) Resveratrol protects myocardial ischemia-reperfusion injury through both NO-dependent and NO-independent mechanisms. *Free Radic. Biol. Med.* 36:774-781
- Itoh Y, Ma FH, Hoshi H, Oka M, Noda K, Ukai Y. (2000) Determination and bioimaging method for

nitric oxide in biological specimens by diaminofluorescein fluorometry. *Anal. Biochem.* 287: 203-209

Je JY, Park JY, Jung WK, Park PJ, Kim SK. (2005) Isolation of angiotensin I converting enzyme (ACE) inhibitor from fermented oyster sauce, *Crassostrea gigas*. *Food Chem.* 90: 809-814

Jin SN, Wen JF, Li X, Kang DG, Lee HS, Cho KW. (2011) The mechanism of vasorelaxation induced by ethanol extract of *Sophora flavescens* in rat aorta. *J. Ethnopharmacol.* 137: 547-552

Kang SM, Heo SJ, Kim KN, Lee SH, Yang HM, Kim AD, Jeon YJ. (2012) Molecular docking studies of a phlorotannin, dieckol isolated from *Ecklonia cava* with tyrosinase inhibitory activity. *Bioorg. & Med. Chem.* 20: 311-316

Ko SC, Kim DG, Han CH, Lee YJ, Lee JK, Byun HG, Lee SC, Park SJ, Lee DH, Jeon YJ. (2012) Nitric oxide-mediated vasorelaxation effects of anti-angiotensin I-converting enzyme (ACE) peptide from *Styela clava* flesh tissue and its anti-hypertensive effect in spontaneously hypertensive rats. *Food Chem.* 134: 1141-1145

Kim HY, Oh H, Li X, Cho KW, Kang DG, Lee HS. (2011) Ethanol extract of seeds of *Oenothera odorata* induces vasorelaxation via endothelium-dependent NO-cGMP signaling through activation of Akt-eNOS-sGC pathway. *J. Ethnopharmacol.* 133: 315-323

Krumenacher JS, Hanafy KA, Murad F. (2004) Regulation of nitric oxide and soluble guanylyl cyclase. *Brain Res. Bull.* 62:505-515

- Lee SH, Han JS, Heo SJ, Hwang JY, Jeon YJ. (2010) Protective effects of dieckol isolated from *Ecklonia cava* against high glucose-induced oxidative stress in human umbilical vein endothelial cells. *Toxicol. In Vitro.* 24:375-381
- Lee SH, Ko CI, Jee Y, Jeong Y, Kim M, Kim JS, Jeon YJ. (2013) Anti-inflammatory effect of fucoidan extracted from *Ecklonia cava* in zebrafish model. *Carbohydr. Polym.* 92: 84-89
- Lorenz M, Wessler S, Follmann E, Michaelis W, Dusterhoft T, Baumann G, Stangl K, Stangl V. (2004) A constituent of Green Tea, Epigallocatechin-3-gallate, Activates Endothelial Nitric oxide synthase by a Phosphatidylinositol-3-OH-kinase-, cAMP-dependent Protein Kinase-, and Akt-dependent Pathway and Leads to Endothelial-dependent Vasorelaxation. *J. Biol. Chem.* 279: 6190-6195
- Martin S, Andriambeloson E, Takeda K, Andriantsitohaina R. (2002) Red wine polyphenols increase calcium in bovine aortic endothelial cells: a basis to elucidate signaling pathways leading to nitric oxide production. *Br. J. Pharmacol.* 135: 1579-1587
- Mount PF, Kemp BE, Power DA. (2007) Regulation of endothelial and myocardial NO synthesis by multi-site eNOS phosphorylation. *J. Mol. Cell. Cardiol.* 42: 271-279
- Park JY, Choi YW, Yun JW, Bae JU, Seo KW, Lee SJ, Park SY, Kim CD. (2012) Gomisins J from *Schisandra chinensis* induces vascular relaxation via activation of endothelial nitric oxide synthase. *Vascul. Pharma.* 57:124-130
- Perola E. (2006) Minimizing false positives in kinase virtual screens. *Proteins.* 64: 422-435

- Rahimi R, Ghiasi S, Azimi H, Fakhari S, Abdollahi M. (2010) A review of the herbal phosphodiesterase inhibitors; Future perspective of new drugs. *Cytokine*. 49: 123-129
- Schwartz BG, Levine LA, Comstock G, Stecher VJ, Kloner RA. (2012) Cardiac Uses of Phosphodiesterase-5 Inhibitors. *J. Am. Coll. Cardiol*. 59: 9-15
- Sung BJ, Hwang KY, Jeon YH, Lee JI, Heo YS, Kim JH, Moon J, Yoon JM, Hyun YL, Kim E, Eum SJ, Park SY, Lee JO, Lee TG, Ro S, Cho JM. (2003) Structure of the catalytic domain of human phosphodiesterase 5 with bound drug molecules. *Nature*. 425: 98-102
- Woldman YY, Sun J, Zweier JL, Khramtsov VV. (2009) Direct chemiluminescence detection of nitric oxide in aqueous solutions using the natural nitric oxide target soluble guanylyl cyclase. *Free Radic. Biol. Med*. 47: 1339-1345
- Yamabe N, Kang KS, Goto E, Tanaka T, Yokozawa T. (2007) Beneficial effect of Corni fructus, a constituent of Hachimi-jio-gan, on advanced glycation endproduct-mediated renal injury in streptozotocin-treated diabetic rats. *Biol. Pharm. Bull*. 30: 520-526

## ACKNOWLEDGEMENT

매년 졸업하시는 선배님들의 논문에 담겨있는 감사의 글을 보면서, 제가 덩달아 감사한 분들을 떠올리며 ‘나중에 꼭 멋진 글을 써야지’ 라는 우습지도 않은 생각을 하곤 했는데, 어느새 시간이 흘러서 석사 졸업을 앞두고 이렇게 글을 쓰고 있습니다. 막상 쓰려고 하니 감사한 분들이 너무 많아 무슨 말을 어떻게 해야 할지 모르겠습니다.

부족한 저에게 관심을 주시고, 연구의 길을 걸을 수 있도록 이끌어주신 전유진 교수님. 실험실에 처음 들어와서부터 지금까지도 변함없이 믿어주시고 기운을 주시는 교수님께 실망시켜 드리지 않으려고, 포기하지 않고 달려왔습니다. 교수님의 믿음과 사랑으로 석사과정을 무사히 마칠 수 있었습니다. 감사합니다. 교수님을 본받아 언제나 변함없이 최선을 다하도록 하겠습니다.

감동적인 수업을 해주셨던 이기완 교수님, 실험실에서 교수님을 뵈 수 있어서 너무 감사했습니다. 제브리피쉬 학회에서 커피 한 캔 사다 주신 마음 따뜻한 송춘복 교수님, 해양생산과학전공에 자부심을 갖고 흥미를 느낄 수 있도록 해주신 최광식 교수님, 부족한 저를 항상 칭찬해주시는 이제희 교수님, 항상 밝은 모습으로 맞아주시는 허문수 교수님, 제 이름을 친근하게 불러주신 이경준 교수님, 영어 공부하도록 동기부여해주신 여인규 교수님, 넘치는 열정으로 가르쳐 주셨지만 최선을 다해 수업에 임하지 못해 죄송했던 김기영 교수님, 언제나 친근하게 대해 주시는 정준범 교수님, 저의 모자란

석사 논문을 심사해주시고, 아낌없이 조언해주신 이승헌 교수님, 발표하는 방법을 가르쳐 주신 정석근 교수님, 앞으로 더 많은 것을 배우고 싶은 박상률 교수님. 해양생명과학과 교수님들께 감사드립니다.

언제나 서로 의지하며 힘든 시간을 버텨온 은아, 아름이 언니, 민영이, 유쾌한 시간을 함께 나누며 파이팅했던 동휘오빠, 승현오빠. 항상 같은 시간에 같은 일을 했었는데, 이젠 그럴 수 없다는 사실이 아쉽기만 합니다. 각자의 선택이 최고의 선택이었음을 증명할 수 있도록 그 곳에서 열심히 하기로 합시다!

언제나 든든하고 멋있는 수진오빠, 실험실을 오가며 많은 도움을 주신 길남오빠, 처음 실험실에 왔을 때 모든 것을 가르쳐 주신 긴내언니, 저를 많이 아껴주셨던 선희언니, 연구원의 자세를 되새기게 해주시는 승홍오빠, 저의 실험 멘토 석천오빠, 모든 것이 완벽한 성명오빠, 잘생긴 한국인 수동오빠, 졸업하고 더 멋있어진 자나카, 친오빠같은 원우오빠, 언제나 열정적인 민철오빠, 마음 편안해지는 주영언니, 항상 밝게 맞아주시는 아름다슬언니, 졸업할 수 있도록 샘플을 분리해 주신 지혁오빠, 동기 같은 재영오빠, 타국 생활이 외롭고, 힘들텐데 도움주지 못한 칼과, 초오빠, 저를 많이 도와준 고마운 현수, 민성, 혜원이, 앞으로 친해져야 하는 윤택이, 서영이. 해양생물자원이용공학 실험실 식구들께 감사드립니다.

못된 친구를 끝까지 품어준 봄이, 선이, 호진이, 유진이, 지은이, 미연이. 고마워! 지금 제출해야 할 시간이라 더 남기지 못해 죄송합니다.

고된 일에 치여 메말라 있을 때마다 단비를 내려주던 Trance 남진오빠, 기철오빠, 하늘이, 정협이. 사랑하는 ACCENT 혜진, 재용, 재혁. 2012년 연말을 함께한 특별한 친구 제영. 귀여운 동생 지민.

석사 졸업 준비하는 사람보다 더 바쁘고 더 고생 많이 한 상원오빠. 오빠의 헌신적인 사랑이 없었으면 불가능했을 것입니다. 너무 고맙습니다.

한 집에 살고 있으면서도 바쁘다는 이유로 언니 노릇 제대로 못해서 너무 미안하지만 고3 수험생활까지 무사히 잘 마친 기특한 우리 동생 나나. 대학에서는 하고 싶은 공부, 하고 싶은 놀이, 하고 싶은 일 하면서 좀 더 활기찬 하루하루를 보낼 수 있도록 해.

제가 하고 있는 일을 존중해주시느라, 못난 딸에게 화 한번 못 내시는 우리 아빠, 엄마. 매일 서운해하시면서도 믿고 지켜봐 주시는 할머니, 할아버지. 혼자 멀리 떨어져 묵묵히 자기 일 열심히 하고 있을 오빠. 언제나 한 가족 우리 고모들. 그 동안 너무 이기적으로 지내온 것 같아 죄송합니다. 그리고 오직 저를 위한 배려와 사랑에 감사드립니다. 제 일을 더 열심히 하는 것이 보답하는 방법이라 생각하며, 최선을 다하겠습니다.